Tectonophysics 612–613 (2014) 56–62

Contents lists available at ScienceDirect

Tectonophysics

journal homepage: www.elsevier.com/locate/tecto

Inelastic response of compliant fault zones to nearby earthquakes in three dimensions

Jingqian Kang *, Benchun Duan

Center for Tectonophysics, Department of Geology & Geophysics, Texas A&M University, College Station, TX, 77843-3115, USA

ARTICLE INFO

Article history:
Received 3 April 2013
Received in revised form 20 November 2013
Accepted 23 November 2013
Available online 4 December 2013

Keywords:
Compliant fault zone
3D inelastic deformation
Near-surface damage
Dynamic rupture simulation
Drucker–Prager yield criteria
Distinguish inelastic from elastic response

ABSTRACT

Using dynamic modeling of earthquake rupture on a strike-slip fault and seismic wave propagation in a three dimensional inhomogeneous elastoplastic medium, we investigate the inelastic response of compliant fault zones to nearby earthquakes. We primarily examine the plastic strain distribution within the fault zone and the displacement field that characterizes the effects of the presence of the fault zone. We find that when the fault zone rocks are close to failure in the prestress field, plastic strain occurs along the entire fault zone near the Earth's surface and some portions of the fault zone in the extensional quadrant at depth, while the remaining portion deforms elastically. Plastic strain enhances the surface displacement of the fault zone, and the enhancement in the extensional quadrant is stronger than that in the compressive quadrant. Inelastic response may be distinguished from elastic response by sympathetic motion (or reduced retrograde motion) exhibited in the fault-parallel horizontal surface displacement in conjunction with enhanced vertical surface displacement in a strike-slip faulting environment. These findings suggest that taking into account both elastic and inelastic deformation of fault zones to nearby earthquakes may improve our estimations of fault zone structure and properties from small-scale surface deformation signals. Furthermore, identifying the inelastic response of nearby fault zones to large earthquakes may allow us to place some constraints on the absolute stress level in the crust.

1. Introduction

Crustal faults are often associated with fractured and damaged rocks around the slip surface. This damage results in a volume of material with increased compliance in the vicinity of the fault, thus creating a compliant fault zone. This increased compliance may result from micro-cracking, coalescence of micro-joints, grain boundary frictional sliding and other microscopic processes during dynamic rupture propagation and stress perturbation (e.g., Chester and Chester, 1998; Chester et al., 1993; Scholz et al., 1993). Seismic trapped waves and travel time analysis have been used to image compliant fault zone geometry (e.g., width and depth) and properties (e.g. rigidity reduction) (e.g., Ben-Zion and Sammis, 2003; Li et al., 1998; Yang et al., 2011). InSAR images of the surface deformation field of large earthquakes have also been studied to infer compliant fault zone structure and properties, primarily based on an elastic inhomogeneous model in which anomalous displacements around a pre-existing fault are considered to be an elastic response of the compliant fault zone to nearby earthquakes (e.g., Barbot et al., 2009; Cochran et al., 2009; Fialko, 2004; Fialko et al., 2002). Although the elastic-response model for anomalous displacements works well in many cases, there are some cases in which mismatch between the prediction from the elastic model and observations is obvious, such as along some displacement profiles across the Calico fault induced by 1992 Mw 7.3 Landers earthquake (Barbot et al., 2009; Cochran et al., 2009).

Vidale and Li (2003) reported that the healing process of the Johnson Valley Fault after the 1992 Mw 7.3 Landers earthquake rupture occurred on it was interrupted by the nearby 1999 Mw 7.1 Hector Mine earthquake. Vidale and Li (2003) proposed that the dynamic stress perturbation from the nearby earthquake may have induced some microscopic processes, such as micro-cracking and/or grain-scale frictional sliding, causing damage of the fault zone rocks. This observation suggests that the response of the fault zone rocks to nearby earthquakes may not be linearly elastic.

The inelastic response of compliant fault zones to nearby earthquakes and the effects on the displacement field in 2D strike-slip faulting models have been studied by Duan and co-workers (Duan, 2010a; Duan et al., 2011). They find that the inelastic response of a compliant fault zone can occur in the extensional quadrant of the nearby rupture when the fault zone rocks are initially close to failure, and that the inelastic response may result in an opposite sense of the horizontal motion across the fault zone with respect to that due to an elastic response in these 2D models. They also point out that neglecting the inelastic response of a compliant fault zone may cause inaccurate estimates of the fault zone structure and properties from observed InSAR displacement fields. However, the InSAR displacement field is dominated by the vertical component, which is absent in these previously published 2D models. How inelastic strain is distributed in the

* Corresponding author. Tel.: +1 979 422 9536.
E-mail addresses: kjq0321@neo.tamu.edu (J. Kang), bduan@tamu.edu (B. Duan).

0040-1951/$ – see front matter © 2013 Elsevier B.V. All rights reserved.
http://dx.doi.org/10.1016/j.tecto.2013.11.033

fault zone and how inelastic response affects the displacement field at the Earth's surface (in particular the vertical component) are important questions, which have significant implications for more accurate estimations of fault zone structure and properties from InSAR images of large earthquakes, and thus for better understanding of fault zone processes and earthquake ruptures. We address the two questions in this three dimensional study.

We remark that compliant fault zones in nature may respond to nearby earthquakes elastically in many cases, as proposed in previous InSAR studies (e.g., Barbot et al., 2009; Cochran et al., 2009; Fialko et al., 2002). However, this study is to explore effects of inelastic response due to dynamic stress perturbations on the displacement field as suggested by Vidale and Li (2003), using dynamic rupture models. Thus, in setting up models, we choose fault zone parameters that are prone to inelastic response. We do not attempt to compare with data in this study, which will be a part of future work.

2. Methodology

We use a community verified finite element code EQdyna (e.g., Duan, 2010a, 2010b; Duan and Day, 2008; Duan and Oglesby, 2006; Duan et al., 2011; Harris et al., 2009, 2011) to perform the numerical simulation of 3D dynamic rupture and seismic wave propagations in inhomogeneous elastoplastic media in this study. A slip weakening friction law (Andrews, 1976; Ida, 1972) is employed to govern the rupture propagation, in which the frictional coefficient drops from static value μ_s to dynamic value μ_d over the critical slip distance D_0 as $\mu(\delta) = \mu_s - (\mu_s - \mu_d)\min\{\delta, D_0\}/D_0$, where δ is the slip on the fault, when shear stress on the fault reaches the yield stress. We choose values for D_0 of 0.4 m, μ_s and μ_d of 0.6 and 0.3, respectively. The fault ends are pinned by a high static frictional coefficient. The dynamic frictional coefficient is linearly tapered from 0.3 to 0.6 at the top and bottom parts of the seismogenic depth to reduce the dynamic stress drop gradually. To initiate the rupture, we prescribe a nucleation patch at the center of the fault plane, within which the rupture is forced to propagate at a fixed slow speed. Outside the nucleation patch, the rupture propagates spontaneously at faster speeds (Fig. 1).

We use the Drucker–Prager yield criterion to describe the material failure in the medium. This criterion (Drucker and Prager, 1952) requires that at a point in the medium, the stress condition satisfies:

$$\sqrt{0.5 s_{ij} s_{ij}} \le -(\sigma_{kk}/3)\sin\varphi + c\cos\varphi \qquad (1)$$

Where s_{ij} is the deviatoric stress, σ_{kk} is the first invariant of the stress tensor, summation over repeated indices is assumed, c is cohesion and φ is the internal frictional angle. The left side of the equation is the square root of the second invariant of the deviatoric stress tensor, which is regarded as a measure of the shear stress in the 3D stress state. The right side of the equation is the yield stress. When the criterion is violated, stresses are adjusted to the yield level. The increments of plastic strain components at one time step $\delta\varepsilon^p_{ij}$ are calculated from the adjustment to the corresponding stress component and shear modulus (e.g., Duan and Day, 2008). Following Ma (2008) and Ma and Andrews (2010), we use a scalar quantity $\eta(t)$ to evaluate the accumulated inelastic strain due to yielding at time t with $\eta(0) = 0$ as follows:

$$\eta(t) = \eta(t-\Delta t) + \delta\eta\Delta t, \qquad \delta\eta = \sqrt{0.5\left(\delta\varepsilon^p_{ij} - \delta\varepsilon^p_{kk}/3\right)\left(\delta\varepsilon^p_{ij} - \delta\varepsilon^p_{kk}/3\right)}. \qquad (2)$$

A depth dependent initial stress field has been assigned over the entire model region. In our coordinate system, the x axis is parallel to the fault plane, the y axis is perpendicular to the fault plane, and the z axis is vertical (Fig. 1). For normal stress, we prescribe σ_{zz} as the effective lithostatic stress σ_{eff} (i.e., $-(\rho - \rho_w)gz = -(16.37\ \text{MPa/km})z$, where ρ and ρ_w are the density of rock and of water, respectively, assuming water level at the free surface, g is the gravitational constant and z is the depth). The sign of stresses has followed the convention in continuum mechanics (i.e., compression is negative); while $\sigma_{xx} = 1.25\sigma_{eff}$, $\sigma_{yy} = 0.75\sigma_{eff}$. For shear stress, we assume $\sigma_{xy} = -0.433\sigma_{eff}$, $\sigma_{xz} = \sigma_{yz} = 0$. This stress state implies the fault plane is optimal in the initial stress field.

We run the dynamic simulations for a sufficient amount of time (i.e., 30 s) to obtain the static deformation field. The main part of the model is surrounded by a much larger buffer region. The buffer region (not shown) is large enough to prevent reflections at artificial model boundaries from contaminating the simulation results. An element size of 100 m in the main model region is used.

3. Models and results

We consider a vertical right-lateral strike-slip faulting regime in a half space in this study (Fig. 1). The fault that ruptures is 20 km long along strike and 15 km wide along dip. We do not include a compliant fault zone surrounding the ruptured fault in the models, as our objective in this study is to investigate the response of a compliant fault zone that

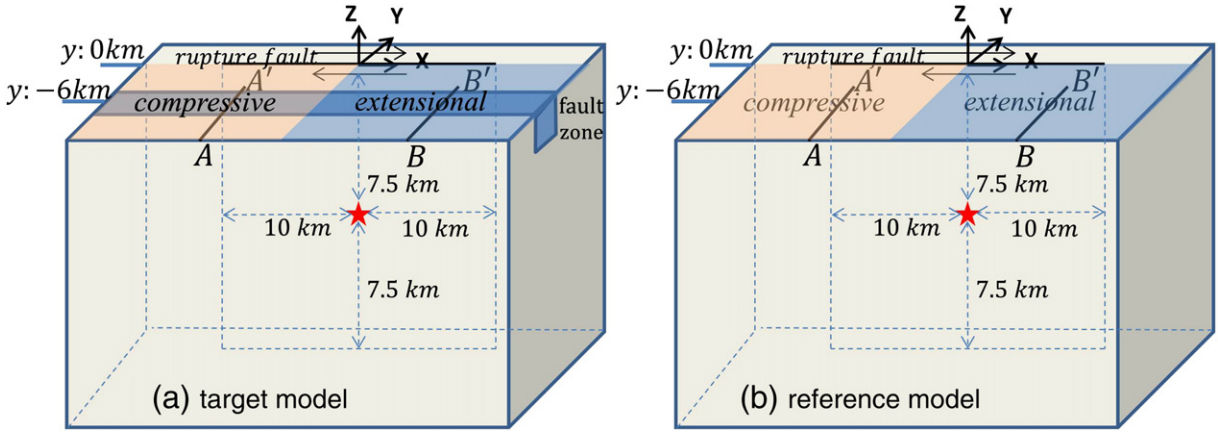

Fig. 1. (a) The target model in this study. The fault that ruptures in the model is 20 km long along strike and 15 km wide along dip. Rupture nucleates at the center of the fault plane, while the epicenter is the origin of the coordinate system. The compliant fault zone is 1.2 km wide and vertically extends to 3 km depth from the Earth's surface and its center is 6 km away from the rupture fault. Seismic velocity within the compliant fault zone has a 40% reduction compared with that in the host rocks. AA′ and BB′ are two profiles shown in Fig. 4. As marked in the figure, AA′ is in the compressive quadrant where it experiences compressive change in the mean stress; while BB′ is in the extensional quadrant where it experiences extensional change in the mean stress. (b) The reference model. The compliant fault zone is excluded but otherwise it is the same as the target model.